

## Spin-Glass Behavior in Frustrated Ising Models with Chaotic Renormalization-Group Trajectories

Susan R. McKay and A. Nihat Berker

*Department of Physics, Massachusetts Institute of Technology, Cambridge, Massachusetts 02139*

and

Scott Kirkpatrick

*IBM Thomas J. Watson Research Center, Yorktown Heights, New York 10598*

(Received 30 December 1981)

Competing ferromagnetic and antiferromagnetic interactions are studied in hierarchical Ising models, which are exactly solvable with nonclassical phase transitions at finite temperature. As model parameters are changed to increase frustration, a spin-glass phase is entered with chaotic renormalization-group trajectories. At successively longer distances, strong and weak spin correlations are encountered in a chaotic sequence. A microscopic description of a spin-glass emerges, with noncontiguous spins mutually pinned within distinct infinite subsets.

PACS numbers: 64.60.-i, 61.40.Df, 05.50.+q, 75.50.Kj

The presence of *frustration*<sup>1</sup> should be essential to unusual cooperative behavior in spin-glasses,<sup>2</sup> since otherwise a gauge transformation recovers an ordinary uniform system. Thus, highly frustrated, but not necessarily random, systems have been the subject of several studies.<sup>3</sup> The present work considers hierarchical Ising models<sup>4</sup> which are frustrated at every length scale. A microscopic characterization of a spin-glass phase emerges, from *chaotic* renormalization-group trajectories.

The hierarchical models<sup>4,5</sup> are exactly solvable models of spins on lattices which are not translationally invariant. They can exhibit nonclassical phase transitions at finite temperatures. A simple example is shown in Fig. 1(a), in which each bond inside the unit in the center is itself actually an entire such unit, and the process is continued *ad infinitum*. The exact renormalization-group transformations for certain hierarchical lattices are algebraically identical to approximate renormalization-group transformations for Bravais lattices, such as the Migdal-Kadanoff bond-moving,<sup>6</sup> Kadanoff variational,<sup>7</sup> and Niemeijer-van Leeuwen cluster<sup>8</sup> schemes. Thus, these are "realizable" approximations<sup>4</sup> and therefore must satisfy basic thermodynamic expectations. Similarly, the present work can be viewed as an exact study of frustration on rather uncommon lattices or as an indirect approximation to frustrated spins on common lattices.

The models analyzed in detail are constructed from the units in Figs. 1(b) and 1(c). Each site  $i$  is occupied by a spin  $\sigma_i = \pm 1$ . The straight lines

represent couplings  $-\beta\mathcal{C}_{ij} = K\sigma_i\sigma_j$ , with  $K \geq 0$ . A wiggly line represents an infinite antiferromagnetic coupling, and has the sole effect of reversing the sign of  $K$  on the bonds adjoining on one side. This is a convenient way of introducing competing ferromagnetic and antiferromagnetic interactions, enabling us to work with one-parameter recursions. Inside the unit of Fig. 1(b),  $p$  bonds are in parallel. This unit is totally frustrated. When  $p_b$  such units are combined in parallel to construct a hierarchical model [Fig. 1(d) with  $p_c = 0$ ], an ordered phase occurs only at intermediate temperatures. As the system is cooled ( $K^{-1} \rightarrow 0$ ), a phase transition occurs from the paramagnetic phase to the ordered phase. Upon further cooling, total frustration effects dominate, and another phase transition occurs from the ordered phase to a *reentrant paramagnetic phase*,<sup>9</sup> which persists to zero temperature. In the unit of Fig. 1(c), at low temperatures, the couplings of the shorter ( $m_1 < m_2$ ) strand dominate, and the longer strand is frustrated. One of the bonds in the longer strand must be dissatisfied, which gives a ground-state entropy of  $\ln m_2$ . At such low temperatures, the spin correlation is still propagated across the unit, although not as the total pinning of ordinary magnets, because of the frustrated longer strand. By contrast, no correlation is propagated at low temperatures across the unit in Fig. 1(b), which produces the reentrance.

A family of hierarchical models is constructed as in Fig. 1(d), taking in parallel  $p_b$  units of Fig. 1(b) and  $p_c$  units of Fig. 1(c). We define the

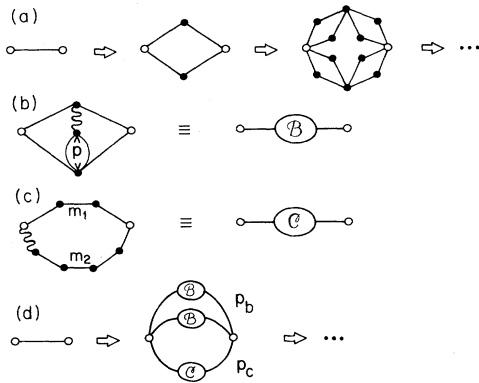


FIG. 1. The construction of hierarchical models.

shortest path across this composite unit as the length rescaling factor of the corresponding renormalization-group transformation,  $b = 2$ . The volume rescaling factor is as usual the ratio of the numbers of old and new bonds,  $b^d = (4 + p)p_b + (m_1 + m_2)p_c$ . This leads to a defined effective dimensionality  $d$ . The average coordination number is

$$\bar{z} = \frac{(4 + p)p_b + (m_1 + m_2)p_c - 1}{2p_b + (m_1 + m_2 - 2)p_c},$$

although smaller and smaller numbers of sites have larger and larger coordinates, a property of hierarchical lattices.

The recursion relations of the corresponding exact renormalization-group transformation are obtained by summing over the internal spins (black circles in Figs. 1) of a composite unit. Thus, with  $t \equiv \tanh K$  and  $\bar{t} \equiv \tanh(pK)$ ,

$$\bar{t}_b = 2t^2(1 - \bar{t}) / (1 + t^4 - 2t^2\bar{t})$$

and

$$K' = p_b \tanh^{-1} \bar{t}_b + p_c (\tanh^{-1} t^{m_1} - \tanh^{-1} t^{m_2})$$

give the renormalized bond strength  $K'$ . The contributions to the free energy from the smaller length scales, which have been traced out by the renormalization transformations, are kept as an additive constant per initial bond to the Hamiltonian  $-\beta\mathcal{H}$ . The recursion for this constant is

$$G' = G + b^{-dn} \left\{ [2p_b + (m_1 + m_2 - 2)p_c] \ln 2 + \frac{p_b}{2} \ln \frac{(1 + t^2)^2 - 4t^2\bar{t}}{(1 - t^2)^2(1 - \bar{t})^2} + \frac{p_c}{2} \ln \frac{(1 - t^{2m_1})(1 - t^{2m_2})}{(1 - t^2)^{m_1 + m_2}} \right\},$$

for the  $n$ th renormalization-group iteration. This quantity converges after many rescalings, giving the free energy per bond of the original system.

We fix the parameters  $p = 4$ ,  $p_c = 1$ , and  $m_1 = m_2 + 1$ , and present results as  $p_b$  or  $m_1$  is scanned, increasing frustration. Figure 2(a) depicts the renormalization-group flows as  $p_b$  is scanned with  $m_1 = 7$ . A stable fixed point always occurs at the decoupled system  $t^* = 0$  and is the sink of

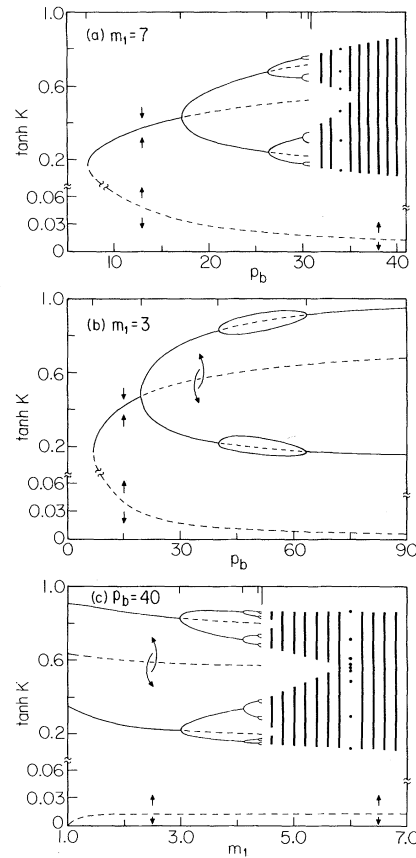


FIG. 2. Renormalization-group topologies as Hamiltonian parameters are scanned. Some of the stable (unstable) fixed points and cycles are shown with full (dashed) lines. Initial bifurcations are noted by tic marks on top of figures. The bigger mark indicates the onset of chaos. Some of the chaotic bands are shown by the vertical segments. The dots illustrate  $6 \times 2^l$ ,  $9 \times 2^l$  cycles in between chaos. Arrows depict renormalization-group flows. The lowest dashed curve is  $t_c^*$ .

the paramagnetic phase. An unstable fixed point occurs at finite coupling  $t_c^*$  and gives a second-order transition between the paramagnetic ( $t < t_c^*$ ) and ordered ( $t > t_c^*$ ) phases. The sink of the ordered phase occurs at stronger coupling. The fact that this sink does not occur at infinite coupling  $t = 1$  reflects ground-state entropy. The novel aspect is the way in which this ordered

sink changes as frustration is increased. At low  $p_b$ , it is a single stable fixed point. At  $p_b = p_b(2^1) \approx 17$ , a period doubling<sup>10</sup> occurs, giving way to a spiral-unstable fixed point and a stable period-2 limit cycle. At  $p_b(2^2) \approx 26$ , another period doubling occurs, giving way to a spiral-unstable period-2 cycle and a stable period-4 limit cycle. The period-doubling cascade proceeds as described in nonlinear mapping contexts.<sup>10</sup> The rate of bifurcation

$$[p_b(2^l) - p_b(2^{l-1})] / [p_b(2^{l+1}) - p_b(2^l)]$$

converges to 4.669... as  $l \rightarrow \infty$ , as predicted by universality.<sup>11</sup> The onset of chaos<sup>10</sup> is at  $p_b(\infty) \approx 31$ . Beyond this value, chaotic bands are encountered [ Fig. 3(a) ] which proceed to merge into an eventual single band [ Fig. 3(b) ], interrupted by small windows of  $9 \times 2^l$ ,  $6 \times 2^l$ , etc. cycles. Similar behavior is exhibited in Fig. 2(c), where  $m_1$  is scanned.

A microscopic interpretation can be given to a chaotic renormalization group. Consider an initial condition in the low-temperature, high-frustration regime. After some renormalizations, the trajectory is confined to the chaotic band. Then, after the  $n_1$ th renormalization, the trajectory will be at a strong-coupling region  $K^{(n_1)} \gg K_c^*$  of the chaotic band. After a few more renormalizations, the trajectory will be at the weaker-coupling  $K^{(n_2)} \sim K_c^*$  region of the band.

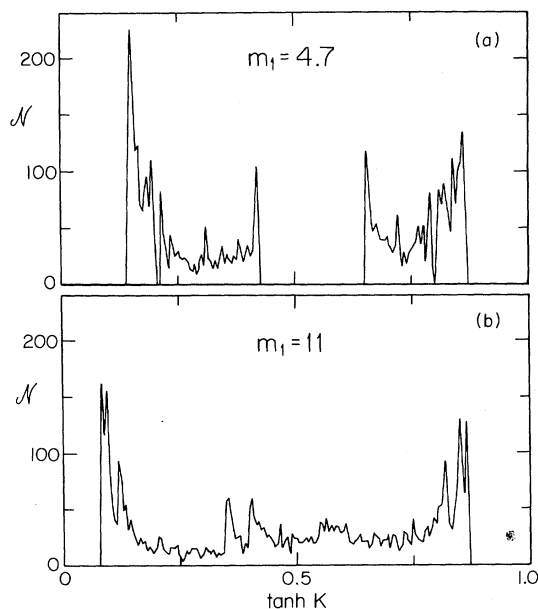


FIG. 3. Number of visits per bin  $\Delta t = 0.05$ , for 5000 chaotic iterations starting at  $t^{(0)} = 0.5$ . The value of  $p_b$  is 40.

After still a few more renormalizations, it will return to the strong-coupling region  $K^{(n_2)} \gg K_c^*$ . Thus, the effective coupling, and therefore the correlation, is strong between spins separated by a length scale  $b^{n_1}$  or  $b^{n_3}$ , whereas the correlation is much weaker between spins separated by  $b^{n_2}$ . As we view successively longer length scales using the renormalization group, we encounter strong and weak correlations in a chaotic sequence. This implies infinite subsets of non-contiguous spins which, within each subset  $s$ , are strongly pinned to each other. The ordering of each subset,  $M_s = \sum_{i \in s} (-1)^{q_i} \sigma_i = \pm M$ , is the ordering of the spin-glass phase. The disorder of the different subsets with respect to each other, and the internal disorder of the finite subsets, provide the entropy of the glass phase. Such non-contiguous pinning has independently been seen in recent Monte Carlo simulation.<sup>12</sup>

In an actual sample, frustration is due to a quenched random spatial distribution of competing interactions. Because of this spatial disorder, different localities will be out of phase with each other with respect to the evolution of local couplings within the chaotic band, under rescaling. The random noise, introduced into the renormalization mapping by the quenched disorder, should wipe out the limit cycles, whereas the chaotic behavior is stable to such noise.<sup>13</sup> A better position-space renormalization-group approximation for a spin-glass on a more realistic lattice would involve trajectories in many-parameter space, again opening an avenue for reaching the chaotic regime without period doubling.

The new renormalization-group behavior described above occurs at the sink of the low-temperature phase. Indeed, the character of the sink (e.g., chaos) should epitomize the entire

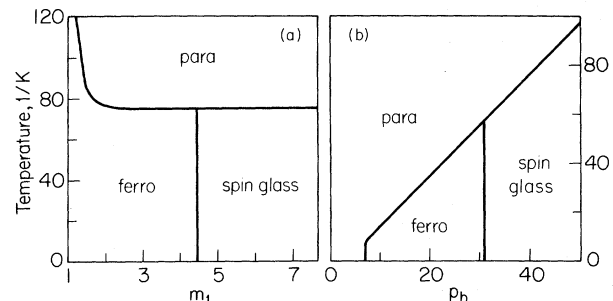


FIG. 4. Phase diagrams deduced from Figs. 2(c) and 2(a).

thermodynamic phase (spin-glass) which is the basin of attraction. In the present work, the phase transition occurs via a standard unstable fixed point  $K_C^*$ , although in many-parameter renormalizations, this could change. The continuum of phase-transition fixed points seen in Figs. 2, between the paramagnetic and spin-glass (chaotic) phases, gives specific-heat exponents  $\alpha$  between  $-6.4$  and  $-6.7$ . This corresponds to a smooth specific-heat signal at the transition, which agrees with spin-glass experiments.<sup>14</sup>

We have presented exact solutions of frustrated hierarchical models that exhibit chaotic renormalization-group trajectories at large frustration. Thus, a microscopic description for spin-glasses is suggested, and phase diagrams are obtained with the expected topology<sup>15</sup> of paramagnetic, ferromagnetic, and spin-glass phases (Fig. 4).

We thank Professor P. C. Martin and Professor D. R. Nelson for introducing us to chaotic phenomena. We acknowledge the hospitality of the University of Maine at Orono (S.R.M.) and of the IBM Thomas J. Watson Research Center (A.N.B.). One of us (A.N.B.) was the recipient of an Alfred P. Sloan Fellowship. This work was supported in part by National Science Foundation Grant No. DMR-79-26405.

<sup>1</sup>G. Toulouse, *Commun. Phys.* **2**, 115 (1977).

<sup>2</sup>S. F. Edwards and P. W. Anderson, *J. Phys.* **F** **5**,

965 (1975). For recent reviews, see *Disordered Systems and Localization*, edited by C. Castellani, C. DiCastro, and L. Peliti (Springer-Verlag, New York, 1981).

<sup>3</sup>J. Villain, *J. Phys. C* **10**, 1717 (1977); G. André, R. Bidaux, J.-P. Carton, R. Conte, and L. de Seze, *J. Phys. (Paris)* **40**, 479 (1979).

<sup>4</sup>A. N. Berker and S. Ostlund, *J. Phys. C* **12**, 4961 (1979).

<sup>5</sup>M. Kaufman and R. B. Griffiths, *Phys. Rev. B* **24**, 496 (1981).

<sup>6</sup>A. A. Migdal, *Zh. Eksp. Teor. Fiz.* **69**, 1457 (1975) [*Sov. Phys. JETP* **42**, 743 (1976)]; L. P. Kadanoff, *Ann. Phys. (N. Y.)* **100**, 359 (1976).

<sup>7</sup>L. P. Kadanoff, *Phys. Rev. Lett.* **34**, 1005 (1975).

<sup>8</sup>T. Niemeijer and J. M. J. van Leeuwen, *Physica (Utrecht)* **72**, 17 (1974).

<sup>9</sup>For another example of a reentrant disordered phase due to spin frustration, in liquid crystals, see A. N. Berker and J. S. Walker, *Phys. Rev. Lett.* **47**, 1469 (1981).

<sup>10</sup>R. B. May and G. F. Oster, *Am. Nat.* **110**, 573 (1976); P. Collet and J.-P. Eckmann, *Iterated Maps on the Interval as Dynamical Systems* (Birkhäuser, Boston, 1980).

<sup>11</sup>M. Feigenbaum, *J. Stat. Phys.* **19**, 25 (1978).

<sup>12</sup>W. Kinzel, to be published.

<sup>13</sup>J. P. Crutchfield and B. A. Huberman, *Phys. Lett. A* **77**, 407 (1980).

<sup>14</sup>J. A. Mydosh, in *Magnetism and Magnetic Materials—1974*, edited by C. D. Graham, G. H. Lander, and J. J. Rhyne, AIP Conference Proceedings No. 24 (American Institute of Physics, New York, 1975), p. 131.

<sup>15</sup>D. Sherrington and S. Kirkpatrick, *Phys. Rev. Lett.* **35**, 1792 (1975).